

Kevin Christmann, Bernd Neubauer, Hartwig Kunanz, Xiang Yong Li, Lin Zhang, Weizhen Xiong, Walter De Queiroz Cassete, Leandro Rocha Martins and Gabriela Ladeira Fajardo

Case Studies of High-Recycling Containing Magnesia-Carbon Bricks in High-Performance Steelmaking Applications

In order to drive sustainability and contribute to ongoing global green steel transformation initiatives, RHI Magnesita has developed tempered magnesia-carbon (MgO-C) bricks with a circular (i.e., recycled) raw material content of up to 30%, showing comparable results to standard high-performance wear lining refractories. This study provides detailed practical examples of such material in use in steel ladle and electric arc furnace applications.

Introduction

The steel industry is globally entering the so-called green steel transformation. Steel producers worldwide are seeking to reduce scope 1 emissions basically by transitioning primary steelmaking from the blast furnace route to electrical steelmaking, with the electric arc furnace (EAF) steelmaking route being combined with hydrogen-based direct reduction. New technical possibilities to reduce CO₂ emissions are being explored all over the steelmaking industry worldwide. Hence, scope 3 emissions are also becoming increasingly important and steel producers are examining the carbon footprint associated with refractory materials, for example tempered MgO-C bricks. Additionally, scrap originating from spent refractory material is causing steel producers issues with regards to landfilling, undesired storage, and logistics costs, as well as potential taxes related to governmental regulations for waste disposal [1,2]. Of course, refractory producers like RHI Magnesita are also looking to reduce scope 1 emissions [3,4].

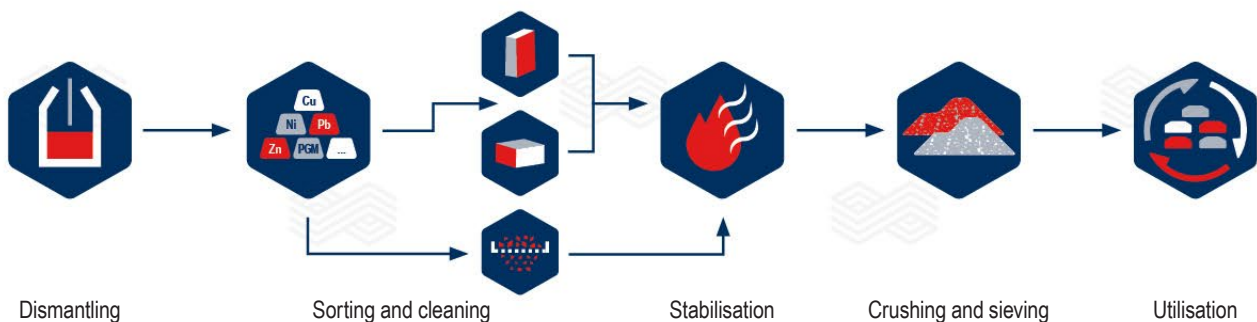
The raw materials in MgO-C bricks are responsible for up to 90% of the total carbon footprint of the final product. That is why, for refractory producers, a major lever to reduce their own scope 1 emissions and contribute to steel producers' efforts in lowering costs and scope 3 emissions is using

circular raw materials in tempered MgO-C bricks at significant amounts of 30% or more. The literature contains many investigations about this type of material, showing positive results [2,5–7]. In addition to the already existing circular raw material containing products for low-wear area applications, RHI Magnesita has developed a new type of product with comparable results to standard high-performance wear lining MgO-C refractories. This study provides detailed practical examples of this material's use in steel ladle and EAF applications.

High-Performance, Tempered MgO-C Refractories Containing Circular Raw Material

Since 2020, RHI Magnesita has globally developed more than 50 tempered MgO-C products containing ≥20% circular raw material for use in steelmaking applications. These products are successfully used in basic oxygen furnaces (BOFs), EAFs, and steel refining ladles in both high- and low-wear areas. The design of these tempered MgO-C products with high amounts of circular raw material requires tight quality control of incoming spent refractory materials and expertise regarding the required processing steps (Figure 1) [5,7].

Figure 1. Processing steps required to reuse spent refractories in MgO-C products [8].



The chemistries of typical circular raw materials used in MgO-C bricks are shown in Table I. These are just examples, demonstrating that there is not one single type, but various types of circular raw material available. This is due to different originating applications (e.g., EAF, BOF, and steel ladle), multiple refractory suppliers, variable presorting in the steel plants, as well as diverse sorting, cleaning, and stabilisation measures in place at different circular raw material suppliers.

The production of MgO-C products with elevated circular raw material content also requires adaptations to the recipe design, as well as the refractory production process itself, to

achieve the necessary physical and chemical properties of the final product. Figure 2 shows the typical microstructure of a tempered MgO-C brick with high circular raw material content (Circular-MgO-C) and a standard product without circular material. As can be seen in Figure 2, the matrix of the Circular-MgO-C shows no significant differences to the standard grade at higher magnification. The graphite is homogeneously distributed in both cases and the matrix filling degree is mid to high. Furthermore, both materials contain the same fused magnesia quality, namely type 97% MgO. At lower magnification, small agglomerations of alumina-based material surrounded by antioxidants can be detected in the Circular-MgO-C (Figure 3).

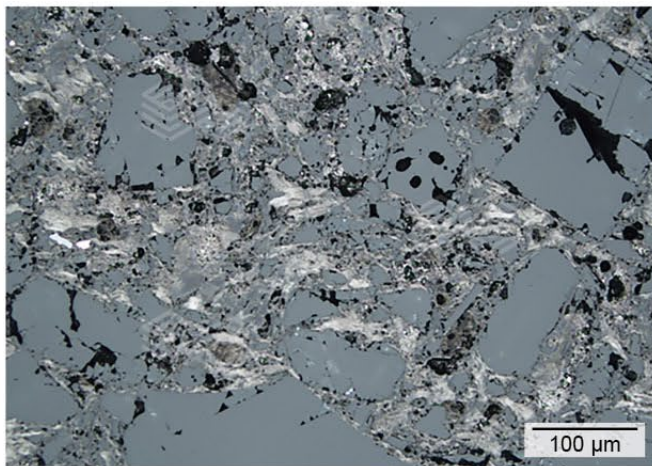
Table I.

Typical chemistry examples of circular raw materials used in MgO-C brick grades.

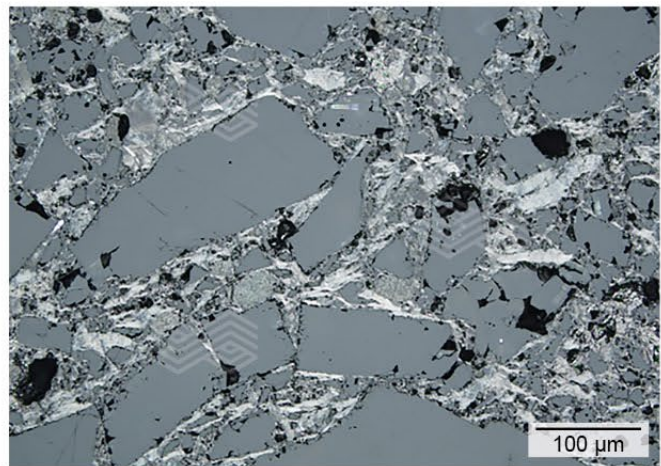
Circular raw material chemistry	MgO [wt.%]	CaO [wt.%]	Fe ₂ O ₃ [wt.%]	Al ₂ O ₃ [wt.%]	SiO ₂ [wt.%]	C [wt.%]
Example 1	94	1.5	1.0	1.0	1	10
Example 2	93	1.5	0.7	1.5	1	10

Figure 2.

Microstructure examples of (a) standard MgO-C and (b) typical Circular-MgO-C bricks.



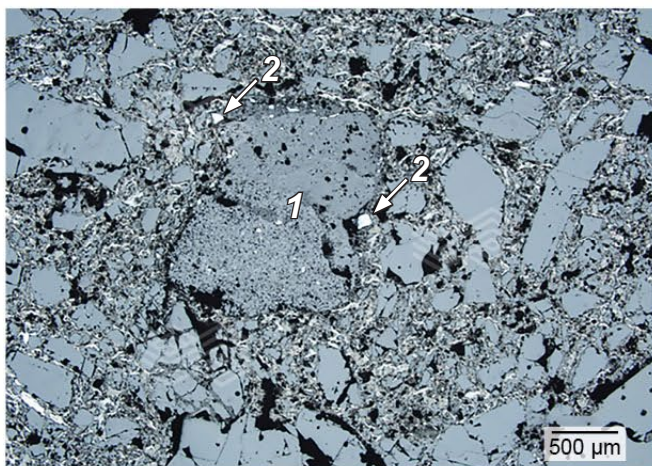
(a)



(b)

Figure 3.

Microstructure of a Circular-MgO-C brick with an alumina-based particle (1) and antioxidants (2).



Case Studies

Case 1: 200-tonne steel ladle slag zone lined with Circular-MgO-C bricks containing 30% circular material

Circular-MgO-C was tested against standard MgO-C bricks in the slag zone of a 200-tonne steel ladle. Both materials had a total carbon content of 14% and no additional antioxidants. The raw material basis of both products was the same, namely fused magnesia type 97% MgO with a lime to silica ratio of 1:1. In the Circular-MgO-C bricks, 30% of the fused magnesia component was replaced with circular raw material. Table II provides a comparison of the chemical and physical properties of both brick types. Clearly, the Al_2O_3 content of the Circular-MgO-C was elevated and although the physical properties after tempering showed a slight

Table II.

Chemical and physical properties of the standard MgO-C and Circular-MgO-C bricks, with the same raw material basis, tested in the steel ladle slag zone. Abbreviations include tonne of CO_2 equivalent per tonne of product (t $\text{CO}_2\text{e/t}$ product).

	Standard MgO-C	Circular-MgO-C
MgO [wt.%]	95.7	93.5
Al_2O_3 [wt.%]	0.5	2.0
Fe_2O_3 [wt.%]	0.8	0.8
CaO [wt.%]	1.5	1.6
SiO_2 [wt.%]	1.5	2.0
C [wt.%]	14.0	14.0
Tempered:		
Bulk density [g/cm^3]	3.02	2.98
Apparent porosity [vol.%]	2.0	2.5
Cold crushing strength [N/mm^2]	45	40
Coked (1000 °C):		
Bulk density [g/cm^3]	2.93	2.94
Apparent porosity [vol.%]	9.5	10
Cold crushing strength [N/mm^2]	30	25
Product carbon footprint [t $\text{CO}_2\text{e/t}$ product]	2.757	2.094

Table III.

Examples of typical ladle slag compositions during the trial period for case study 1.

	MgO [wt.%]	Al_2O_3 [wt.%]	SiO_2 [wt.%]	CaO [wt.%]	TiO_2 [wt.%]	Cr_2O_3 [wt.%]	MnO [wt.%]	Fe_2O_3 [wt.%]	B4
Ladle slag (Al-killed)	1.55	21.22	13.64	62.48	0.26	0.11	0.14	0.33	1.84
Ladle slag (Si-killed)	8.45	12.60	31.46	18.38	2.42	0.32	15.37	10.33	0.61

deterioration compared to the standard material, after coking the values were comparable. The product carbon footprint was calculated according to ISO 14067 [9].

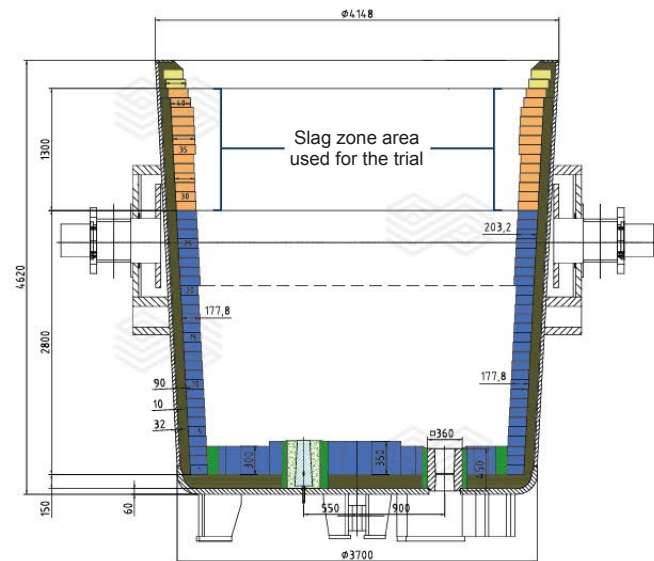
The steel plant operates two 190-tonne BOFs and a ladle furnace, as well as one billet caster. The product portfolio consists mainly of structural steel, with the share between Al-killed and Si-killed steel being approximately 70% and 30%, respectively. Table III shows typical examples of Al-killed and Si-killed steel ladle slags from this plant, which can be highly aggressive against basic refractories.

In Figure 4 the slag zone area (layer 29–41), where the standard MgO-C and Circular-MgO-C bricks were tested, is indicated in orange. The barrel and bottom were lined with alumina-magnesia-carbon (AMC) bricks. The slag zone lining was designed with MK8 and MK9 mini key shapes, with a thickness of 203.2 mm and 228.6 mm, respectively.

In total three sets of the Circular-MgO-C bricks were tested and the results compared to standard MgO-C material. The

Figure 4.

200-tonne steel ladle lined with 14% carbon-containing MgO-C in the slag zone.



target lifetime of the ladles running in this plant is 75 heats, which was achieved by the ladles equipped with the Circular-MgO-C. Figure 5 shows a comparison between the standard and Circular-MgO-C bricks at 73 and 75 heats, respectively.

There was no difference in maintenance schedules for the standard and Circular-MgO-C lined steel ladles. The average wear rate of the Circular-MgO-C was 2.07 mm/heat, compared to 2.02 mm/heat for the standard bricks. This very minor difference in performance, combined with a 9% cost decrease and 24% CO₂ equivalent reduction, led to the decision to completely replace the standard slag zone material with Circular-MgO-C.

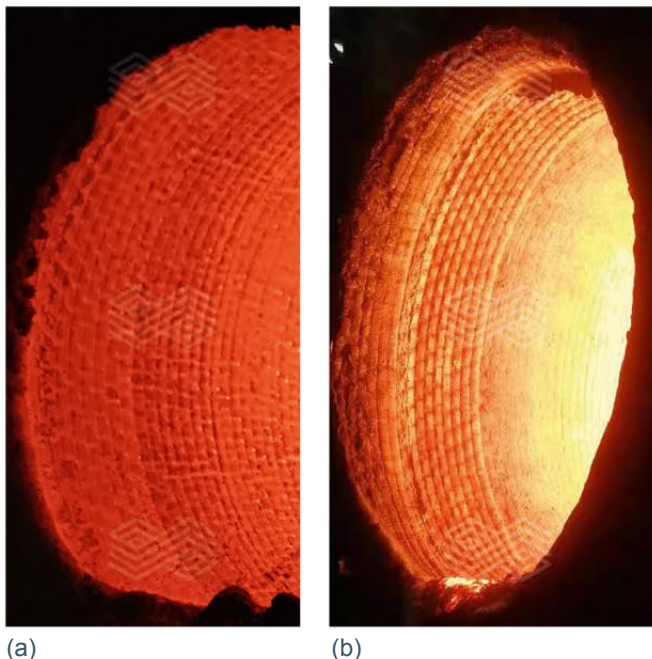
Case 2: 340-tonne steel ladle slag zone (upper and lower part) lined with two types of Circular-MgO-C bricks containing 20% circular material

Two Circular-MgO-C brick grades were tested in 340-tonne steel ladles against standard MgO-C materials. At this steel plant the steel ladle slag zone is separated into high- and low-wear areas. For the high-wear area bricks, a fused magnesia type with 98% MgO was used while for the low-wear area a fused magnesia type with 97% MgO was selected. The corresponding Circular-MgO-C in both areas had the same fused magnesia basis. The total carbon content of all the materials was 12%.

Table IV and Table V provide a comparison of the two Circular-MgO-C brick grades with the equivalent standard MgO-C materials for the high- and low-wear areas of the steel ladle slag zone. As in the material comparison described for case 1, differences between the standard and Circular-MgO-C bricks were mainly the Al₂O₃ content and physical properties after tempering. However, the typical coked values for both the high- and low-wear area

Figure 5.

(a) standard bricks at 73 heats and (b) Circular-MgO-C bricks at 75 heats in the slag zone of a 200-tonne steel ladle.



Circular-MgO-C materials were similar to the standard materials, and for the low-wear area the density of the Circular-MgO-C material was even higher than the standard MgO-C. The carbon footprint reduction was 37% and 13% for the high- and low-wear area Circular-MgO-C materials, respectively.

Table IV.

Chemical and physical properties of the standard MgO-C and Circular-MgO-C bricks, with the same raw material basis, tested in the high-wear area of the steel ladle slag zone. Abbreviations include tonne of CO₂ equivalent per tonne of product (t CO₂e/t product).

	Standard MgO-C	Circular-MgO-C
MgO [wt. %]	97.4	95.3
Al ₂ O ₃ [wt. %]	0.2	0.9
Fe ₂ O ₃ [wt. %]	0.6	1.5
CaO [wt. %]	1.1	1.2
SiO ₂ [wt. %]	0.6	0.8
C [wt. %]	12.0	12.0
Tempered:		
Bulk density [g/cm ³]	3.06	3.08
Apparent porosity [vol. %]	3.0	3.0
Cold crushing strength [N/mm ²]	50	50
Coked (1000 °C):		
Bulk density [g/cm ³]	2.97	2.96
Apparent porosity [vol. %]	10.0	10.8
Product carbon footprint [t CO ₂ e/t product]	2.977	1.887

Table V.

Chemical and physical properties of the standard MgO-C and Circular-MgO-C bricks, with the same raw material basis, tested in the low-wear area of the steel ladle slag zone. Abbreviations include tonne of CO₂ equivalent per tonne of product (t CO₂e/t product).

	Standard MgO-C	Circular-MgO-C
MgO [wt. %]	97.0	95.9
Al ₂ O ₃ [wt. %]	0.2	0.9
Fe ₂ O ₃ [wt. %]	0.6	0.8
CaO [wt. %]	1.3	1.5
SiO ₂ [wt. %]	0.7	0.9
C [wt. %]	12.0	12.0
Tempered:		
Bulk density [g/cm ³]	3.06	3.04
Apparent porosity [vol. %]	3	4.5
Cold crushing strength [N/mm ²]	50	43
Coked (1000 °C):		
Bulk density [g/cm ³]	2.94	2.97
Apparent porosity [vol. %]	10.5	9.0
Product carbon footprint [t CO ₂ e/t product]	2.832	2.463

This steel plant operates two 340-tonne BOFs, two ladle treatment stations, one aluminothermal heating station (on average 50% of the total heats per ladle), two RH degassers (on average 50% of the total heats per ladle), and two continuous casters. The plant produces construction and automotive steel, as well as steel for domestic appliances, agribusiness, and the energy sector. The steel is 100% Al-killed and Table VI shows the chemistry of a typical steel ladle slag.

During the trials it was possible to directly compare the Circular-MgO-C and standard bricks in the same lining (Figure 6). As can be seen in Figure 6, the standard materials were installed on the right-hand side from layer 12–19 for the low-wear area, indicated in yellow (152 mm lining thickness), and layer 20–27 for the high-wear area, denoted by purple (152 mm and 178 mm lining thickness), in 180° of the ladle lining. On the opposite side of the standard material, a 180° panel of the Circular-MgO-C materials was installed in the high-wear area, marked blue, and the low-wear area, indicated in green. In total 3 trials were conducted with the circular material, and in the 3rd trial the entire slag zone (360°) was lined with Circular-MgO-C.

Figure 6.
Steel ladle lining setup to directly compare the Circular-MgO-C and standard MgO-C bricks.

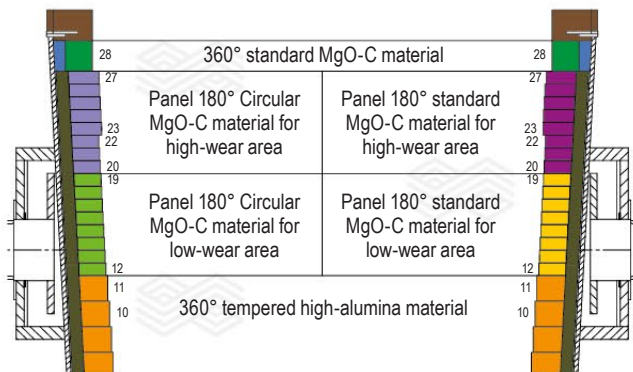


Figure 7 shows a direct comparison of the Circular-MgO-C and the standard MgO-C materials during a ladle campaign. As can be seen, the Circular-MgO-C behaved in a similar manner to the standard MgO-C. The target lifetime at this

Figure 7.
Steel ladle campaign showing the slag zone (high- and low-wear areas) lined with Circular-MgO-C on the left-hand side and the standard MgO-C on the right-hand side of the blue bar.

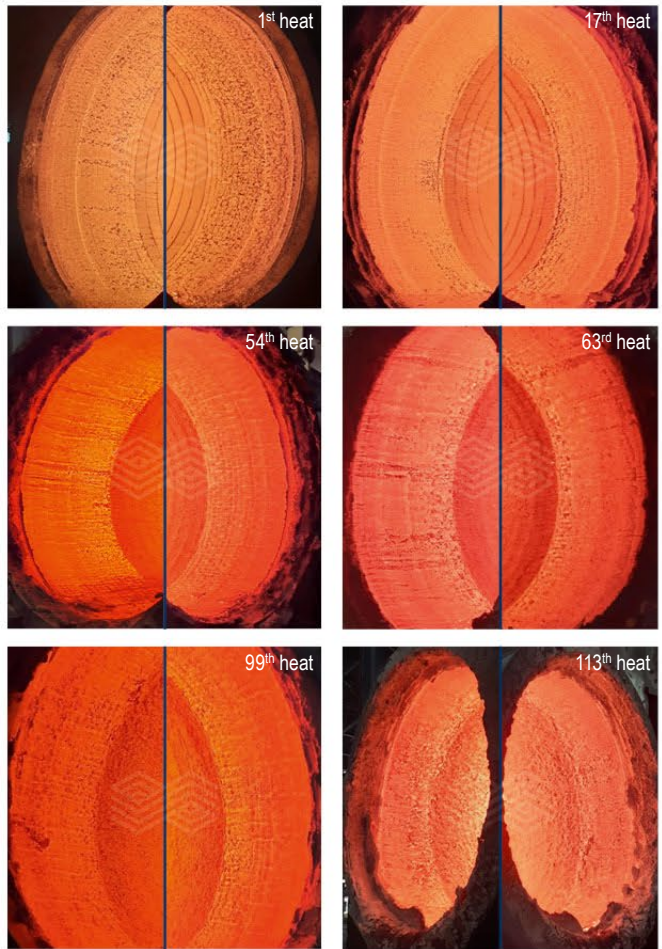


Table VI.
Example of a typical ladle slag composition during the trial period for case study 2.

	MgO [wt.%]	Al ₂ O ₃ [wt.%]	SiO ₂ [wt.%]	CaO [wt.%]	P ₂ O ₅ [wt.%]	MnO [wt.%]	Fe total [wt.%]	S [wt.%]	TiO ₂ [wt.%]	B4
Ladle slag (Al-killed)	9.61	29.85	5.19	50.45	0.08	1.45	1.18	0.16	0.29	1.71

steel plant is 120 heats for the steel ladles, which was achieved by the Circular-MgO-C bricks. Figure 8 shows a typical tear out profile of the slag zone lined with Circular-MgO-C bricks.

The average wear rates of the standard and Circular-MgO-C materials in the high-wear area were 1.04 and 1.05 mm/heat, respectively. For the low-wear area, the average wear rate for the standard material was 0.55 mm/heat, while the Circular-MgO-C in this area achieved on average 0.64 mm/heat. Since the target was 120 heats and a minimum safety thickness of 40 mm is demanded, the requirements were achieved with the Circular-MgO-C. With regards to gunning maintenance, the ladles lined with circular material in the slag zone had a specific consumption of 0.30 kg/tonne_{steel} while the historical specific consumption was 0.28 kg/tonne_{steel}. The combination of both Circular-MgO-C bricks reduced the carbon footprint of the steel ladle slag zone by 26%. The plant has shifted to operating 25% of the steel ladle slag zones with Circular-MgO-C.

Figure 8.

Typical tear-out profile of a Circular-MgO-C slag zone.



Case 3: 35-tonne EAF slag zone lined with Circular-MgO-C bricks containing 30% circular material

In the third case study, Circular-MgO-C based on a fused magnesia type with 97% MgO was tested in the slag zone of a 35-tonne EAF. The standard MgO-C material had the same fused magnesia basis. Both materials had a total carbon content of 10%. Table VII provides a comparison of the Circular-MgO-C and standard MgO-C materials, with regards to their chemistry and physical properties. The comparison in Table VII shows that in this case the differences between the standard MgO-C and Circular-MgO-C bricks were significant, not only regarding the Al₂O₃ content, but especially the bulk density and porosity. Unlike in the other 2 cases presented, the coked values of the Circular-MgO-C and the standard MgO-C material were not on a comparable level.

Table VII.

Chemical and physical properties of the standard MgO-C and Circular-MgO-C bricks, with the same raw material basis, tested in the EAF slag zone. Abbreviations include tonne of CO₂ equivalent per tonne of product (t CO₂e/t product).

	Standard MgO-C	Circular-MgO-C
MgO [wt.%]	97.0	95.6
Al ₂ O ₃ [wt.%]	0.5	1.5
Fe ₂ O ₃ [wt.%]	0.6	0.7
CaO [wt.%]	1.3	1.5
SiO ₂ [wt.%]	0.6	0.9
C [wt.%]	10.0	10.0
Tempered:		
Bulk density [g/cm ³]	3.14	3.05
Apparent porosity [vol.%]	3.7	5.5
Cold crushing strength [N/mm ²]	50	45
Coked (1000 °C):		
Bulk density [g/cm ³]	3.08	2.98
Apparent porosity [vol.%]	8.0	9.5
Product carbon footprint [t CO ₂ e/t product]	2.646	2.139

This steel plant is mainly producing stainless steel. The steel plant has two 35-tonne EAFs, one 90-tonne argon oxygen decarburization (AOD) converter, one 80-tonne oxygen blowing furnace (OBF), one 80-tonne hot metal treatment station, one 90-tonne ladle furnace, two 80-tonne vacuum oxygen decarburization (VOD) units, and two continuous casters. The EAF in this steel plant melts scrap, including ferrochrome, and feeds the AOD and OBF with this so-called premelt. A typical EAF slag composition at this plant is shown in Table VIII.

The Circular-MgO-C bricks were installed in the EAF slag zone (350 mm lining thickness), entirely replacing the standard MgO-C material in this area. Figure 9 shows this EAF slag zone in a light blue colour. In total three trial campaigns were run with the Circular-MgO-C material and after each campaign the remaining brick thickness was measured during the wrecking (Figure 10). The minimum lifetime requirement at this EAF plant is 600 heats and the Circular-MgO-C containing vessels achieved on average 680 heats. The wear rate of the standard MgO-C material was on average 0.17 mm/heat, whereas the Circular-MgO-C material achieved an average of 0.19 mm/heat. Furthermore, the gunning maintenance for the 3 trial campaigns was not increased. By using the Circular-MgO-C material, the carbon footprint of the slag zone was reduced by 19% and the steel plant has already switched one EAF entirely to the Circular-MgO-C bricks in the slag zone.

Figure 10.

(a–b) dismantling the EAF refractory lining and (c–e) wear rate measurements of the slag zone Circular-MgO-C bricks.



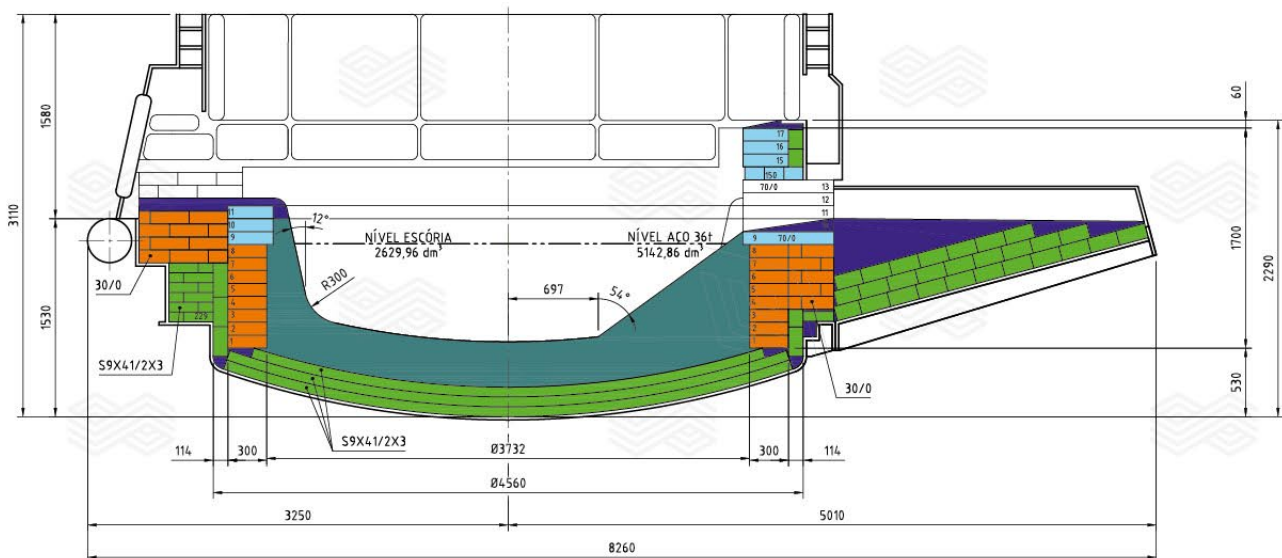
Table VIII.

Example of a typical EAF slag composition during the trial period for case study 3.

	MgO [wt.%]	Al ₂ O ₃ [wt.%]	SiO ₂ [wt.%]	CaO [wt.%]	Cr ₂ O ₃ [wt.%]	MnO [wt.%]	FeO [wt.%]	B4
EAF slag	12.08	11.09	29.38	40.78	3.61	1.31	1.75	1.31

Figure 9.

35-tonne EAF refractory lining design with the Circular-MgO-C bricks in the slag zone indicated with a light blue colour.



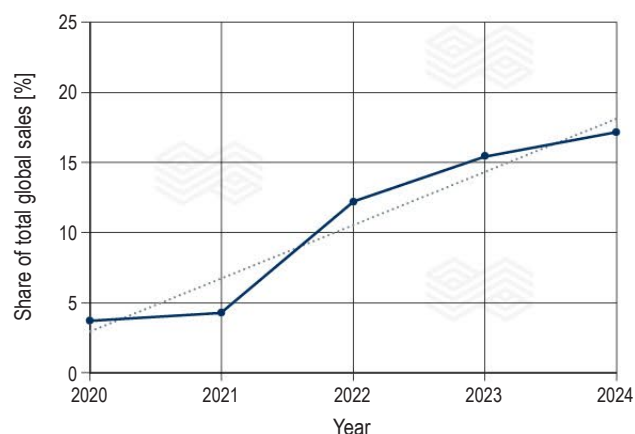
Summary and Conclusion

In this article, three different case studies have been presented where standard MgO-C was replaced by Circular-MgO-C bricks in high-wear areas. The trials covered different steel plants and applications (i.e., EAF and steel ladle), including Al- and Si-killed steels. In all cases, the Circular-MgO-C material significantly reduced the carbon footprint while achieving comparable wear rates to the standard material, even in highly aggressive environments. Furthermore, the Circular-MgO-C has replaced the corresponding standard MgO-C materials for regular production. The global success of these new types of high-performance Circular-MgO-C bricks is mirrored in the development of shipments (Figure 11). From 2020 to the end of 2023, the volumes sold have steadily increased and the share of total global sales for these high-performance Circular-MgO-C will reach 20% in 2024. It is expected that this trend will further accelerate globally, with the increasing need to reduce CO₂ emissions, avoid landfilling, and additional costs for storage and logistics of spent refractory materials.

In conclusion, the trials described in this article demonstrate that MgO-C bricks based on circular raw materials are suitable for high-wear areas and aggressive environments. Furthermore, even with a circular raw material content of up to 30%, the latest generation of Circular-MgO-C bricks developed by RHI Magnesita achieves performance comparable to standard MgO-C material, along with significant CO₂ savings.

Figure 11.

Increased global sales of high-performance Circular-MgO-C bricks since 2020 (solid line) and the average share of total global sales (dotted line).



References

- [1] Horckmans, L., Nielsen, P., Dierckx, P. and Ducastel, A. Recycling of Refractory Bricks Used in Basic Steelmaking: A Review. *Resources, Conservation and Recycling*. 2019, 140, 297–304.
- [2] Moritz, K., Dudczig, S., Endres, H.G., Herzog, D., Schwarz, M., Schöttler, L., Veres, D. and Aneziris, C.G. Magnesita-Carbon Refractories from Recycled Materials. *International Journal of Ceramic Engineering & Science*. 2022, 4, 53–58.
- [3] <https://www.rhimagnesita.com/our-sustainability/>
- [4] RHI Magnesita 2023 Sustainability Report. <https://www.rhimagnesita.com/wp-content/uploads/2024/04/rhim-sustainability-report-2023-final-2.pdf>
- [5] Ludwig, M., Śnieżek, E., Jastrzębska, I., Prorok, R., Sułkowski, M., Gołowski, C., Fischer, C., Wojteczko, K. and Szczerba, J. Recycled Magnesita-Carbon Aggregate as the Component of New Type of MgO-C Refractories. *Construction and Building Materials*. 2021, 272, 121912.
- [6] Moritz, K., Kerber, F., Dudczig, S., Schmidt, G., Schemmel, T., Schwarz, M., Jansen, H. and Aneziris, C.G. Recyclate-Containing Magnesita-Carbon Refractories – Influence on the Non-Metallic Inclusions in Steel. *Open Ceramics*. 2023, 16, 100450.
- [7] Kunanz, H., Nonnen, B., Kirowitz, J. and Schnalzger, M. Successful Implementation of a High Recycling Containing Magnesita-Carbon Brick in Steel Ladles. *Bulletin*. 2022, 17–20.
- [8] Moraes, M., Leitner, A., Nogueira, G., Zocratto, B., Heid, S. and Mühlhäußer, J. Technical Challenges for Refractory Recycling and Innovative Processing Solutions. *Bulletin*. 2023, 33–38.
- [9] Joos-Bloch, M., Rechberger, L., Haider, C., Moulin-Silva, W., Wucher, J. and Drnek, T. Product Carbon Footprint of Refractory Products. *Bulletin*. 2023, 39–44.

Authors

Kevin Christmann, RHI Magnesita, Wiesbaden, Germany.
 Bernd Neubauer, RHI Magnesita, Leoben, Austria.
 Hartwig Kunanz, RHI Magnesita, Leoben, Austria.
 Xiang Yong Li, RHI Magnesita, Dalian, China.
 Lin Zhang, RHI Magnesita, Dalian, China.
 Weizhen Xiong, RHI Magnesita, Dalian, China.
 Walter De Queiroz Cassete, RHI Magnesita, Contagem, Brazil.
 Leandro Rocha Martins, RHI Magnesita, Contagem, Brazil.
 Gabriela Ladeira Fajardo, RHI Magnesita, Contagem, Brazil.

Corresponding author: Kevin Christmann, Kevin.Christmann@rhimagnesita.com



Bulletin

The Journal of Refractory Innovations

2024

Published by
Chief Editor
Executive Editors

RHI Magnesita GmbH, Vienna, Austria
Thomas Prietl

Celio Carvalho Cavalcante, Thomas Drnek, Christoph Eglssäer, Celso Freitas,
Alexander Leitner, Ravikumar Periyasamy, Stefan Postrach, Peter Steinkellner,
Karl-Michael Zettl

Raw Materials Expert
Technical Proofreader
Lingual Proofreader
Project Manager
Design and Typesetting

Matheus Naves Moraes
Clare McFarlane
Clare McFarlane
Michaela Hall
Universal Druckerei GmbH, Leoben, Austria

Contact

Michaela Hall
RHI Magnesita GmbH, Technology Center
Magnesitstrasse 2
8700 Leoben, Austria

E-mail

bulletin@rhimagnesita.com

Phone

+43 50213 5300

Website

rhimagnesita.com

LinkedIn

<https://www.linkedin.com/company/rhi-magnesita>

The products, processes, technologies, or tradenames in the Bulletin may be the subject of intellectual property rights held by RHI Magnesita N.V., its affiliates, or other companies.

The texts, photographs and graphic design contained in this publication are protected by copyright. Unless indicated otherwise, the related rights of use, especially the rights of reproduction, dissemination, provision and editing, are held exclusively by RHI Magnesita N.V. Usage of this publication shall only be permitted for personal information purposes. Any type of use going beyond that, especially reproduction, editing, other usage or commercial use is subject to explicit prior written approval by RHI Magnesita N.V.

Cover picture: The image depicts the lower section of a RH degasser, a secondary metallurgical unit used in steel plants. In the RH degassing process, snorkels are submerged into liquid steel contained in the casting ladle. Argon gas is purged through the inlet snorkel, creating a suction effect that draws liquid steel into the lower vessel of the RH degasser, where a vacuum is applied. The steel treated in the lower vessel flows back to the ladle through the outlet snorkel, creating a continuous steel circulation between the ladle and the RH degasser. The strong negative pressure (vacuum) within the RH degasser facilitates various metallurgical processes that enhance steel quality, with the key process steps including degassing, decarburisation, deoxidation, and alloying under vacuum. Rail steel, flat steel for the automotive industry, and steel plates for shipbuilding are just a few examples of products that benefit from the RH degasser. Prefabricated snorkels, which RHI MAGNESITA manufactures ready for use and delivers to our globally operating customers, are essential components of the RH degasser.